Supplementary Information (SI) for Journal of Materials Chemistry A.

# Supporting Information

## Anionic Leaching Induced Amorphous Cu/CuOx on N-doped Carbon for Efficient Electrochemical Nitrate Reduction to Ammonia

Maolin Zhang,[2,†] Karthik Peramaiah,[3,†] Muyu Yi,[4] and Hao Huang[1,*]

[1] Nano Science and Technology Institute, Suzhou Institute for Advanced Research, University of Science and Technology of China, Suzhou 215123, China

[2] Institute of Environment and Sustainable Development in Agriculture, Chinese Academy of Agricultural Sciences, Beijing 100081, China

[3] Institute of Sustainability for Chemicals, Energy, and Environment (ISCE2), Agency for Science, Technology, and Research (A*STAR), Singapore 627833, Singapore

[4] Chemistry Program, Center for Renewable Energy and Storage Technologies (CREST) and Division of Physical Sciences and Engineering, King Abdullah University of Science and Technology, Thuwal 23955-6900, Saudi Arabia

[†] Those authors contributed equally to this work

[*] Corresponding author: Hao Huang (haohuang@ustc.edu.cn)

## Reagents and Materials

All chemicals were used as received without further purification. $CuCl_2\cdot 2H_2O$ (≥99.95%), $CuSO_4\cdot 5H_2O$ (≥98%), KBr (≥99%), KI (≥99.0%), dicyandiamide (≥99%), citric acid (≥99.5%), $NaBH_4$ (≥98%), $KNO_3$ (≥99.0%), KOH (≥99.95%), ethanol (≥99.95%), Nafion, salicylic acid, sodium citrate, NaClO, $C_5FeN_6Na_2O$, indophenol, $NH_4Cl$, para-(dimethylamino) benzaldehyde, and carbon black (batch number:699632) were purchased from Sigma-Aldrich. Sustainion® XA-9 ionomer solution, reinforced Sustainion® 37-50 proton exchange membrane, and $NiFeO_x$ catalyst were purchased from Dioxide Materials (FL, USA). Bipolar membrane (Xion BPM-Aquivion-870-Durion-LMW-30μm, model 590642) and Toray carbon paper (AvCarb p75T-Wet Proof) were purchased from Fuel Cell Store (Texas, USA).

## Synthesis of the catalysts

Nitrogen doped Carbon Black (N/CB) was synthesized by mixing 0.5 g of CB with 0.5 g of dicyandiamide and then calcined at 800 °C in nitrogen atmosphere for 2 hours with a heating rate of 2 °C $min^{-1}$. In a typical synthesis of CuCl-N/CB, 2 mmol of $CuCl_2\cdot 2H_2O$, 100 mg of citric acid, 50 mg of N/CB were mixed in 20 mL of DI water. 10 mL of $NaBH_4$ solution (0.1 M) was slowly added into the previously solution and kept stirring at 20 °C for 10 min. The product was purified by deionized water several times to remove the unreacted precursors, collect by vacuum filtration, and dried under a vacuum overnight. The obtained powder was CuCl-N/CB, respectively. CuBr-N/CB and CuI-N/CB were synthesized in a similar way by replacing $CuCl_2\cdot 2H_2O$ with same mole of $CuSO_4\cdot 5H_2O$ and KBr/KI, respectively.

Compared with the synthesis of CuCl-N/CB sample, the CuCl-N/CB (10%) sample was synthesized in a similar way by reducing the quality of $CuCl_2\cdot 2H_2O$ to 0.2 mmol and $NaBH_4$ solution (0.1 M) to 1 mL. The CuCl-N/CB (150%) sample was synthesized by increasing the quality of $CuCl_2\cdot 2H_2O$ to 3 mmol and $NaBH_4$ solution (0.1 M) to 15 mL, respectively. Pure CuCl sample was synthesized in a similar procedure without adding N/CB. The $CuO_x$-N/CB sample was synthesized in a similar procedure by increasing the $NaBH_4$ concentration to 1 M, respecively.

## Characterizations

Powder X-ray diffraction patterns (PXRD) were recorded with a Bruker D8 Advance X-ray powder diffractometer with monochromatized Cu Kα radiation (λ = 1.5418 Å) using LynxEye 1D detector. The diffractometer operating conditions were 40 mA, and 40 kV at room temperature. HAADF-STEM and X-ray energy dispersive spectroscopy (EDS) elemental mapping were carried out on a probe Cs-corrected FEI-ST Titan 80-300 kV (ST) microscope using Ni-based TEM grids. TEM analysis was carried out by operating the microscope at an operating voltage of 300 kV. Inductively coupled plasma optical emission spectrometry (ICP-OES) was performed on Thermo Fisher IRIS Intrepid Ⅱ. X-ray photoelectron spectroscopy (XPS) studies were carried out in a Kratos Axis Ultra DLD spectrometer equipped with a monochromatic Al *K*α X-ray source (h*v* = 1486.6 eV) operating at 150 W, a multichannel plate and delay line detector under a vacuum of $1{\sim}10^{-9}$ mbar. The high-resolution spectra were collected at fixed analyzer pass energies of 20 eV. The sample was mounted in the floating mode in order to avoid differential charging. Charge neutralization was required for all samples. Binding energies were referenced to the $sp^3$-hybridized (C-C) carbon for the C 1s peak set at 284.8 eV. The absorption spectrum by the indophenol blue method was measured using a UV-vis spectrophotometer (UV-Vis-NIR-Lambda 950_acl).

## Electrocatalyst reduction of $NO_3^-$ in H-cell.

To prepare cathodic electrode, the obtained 5 mg of catalyst was dispersed in 720 µL of ethanol, 240 µL of deionized water, and 40 µL of 5 wt% Nafion solution with sonication for 30 min, then 50 µL of the mixed solution was dropped on 1×1 $cm^2$ carbon paper and dried at room temperature. The loading amount of the catalyst is 0.25 mg $cm^{-2}$. The electrocatalytic experiment was carried out with a potentiostat

(Biologic-VMP3) in a two-compartment electrochemical cell, and a bipolar membrane was used to separate the anodic and cathodic compartments. The catalyst-loaded carbon paper and an Ag/AgCl (saturated KCl solution) were placed on the cathodic side and used as the working and reference electrode, respectively. A platinum wire electrode was used as the counter electrode on the anodic side. For the cathodic compartment, a mixture of 0.1 M $KNO_3$ and 1 M KOH electrolyte was used, while the anodic compartment was 1 M of KOH electrolyte. Each compartment contained 40 mL of electrolyte. The cathodic electrolyte was pre-saturated with Ar (99.999%) with an average flow rate of 10 sccm for 30 min. The pH of the electrolyte was measured to be 14 using the pH indicator paper (Whatman$^{TM}$). Cyclic voltammetry (CV) and polarization curves were collected (no iR-corrected) at a scan rate of 5 mV $s^{-1}$ using potentiostat (Biologic-SAA). For the catalyst activation, a 15-cycle CV test was conducted from 1.04 V to -0.46 V vs RHE. Then $NO_3^-$RR was performed with chronoamperometry measurement at each fixed potential for 0.5 h.

**Electrocatalytic reduction and solar-driven reduction of $NO_3^-$ by the proton exchange membrane electrolyzer.**

The $NiFeO_x$ was used as anode OER catalyst. The commercial reinforced Sustainion® proton exchange membrane was used in the middle between anode and cathode. To prepare the cathodic electrode, the obtained 5 mg of catalyst was dispersed in 720 µL of ethanol, 240 µL of deionized water, and 40 µL of Sustainion® XA-9 ionomer solution with sonication for 30 min, then 500 µL of the mixed solution was dropped on 2.25 × 2.25 cm carbon fiber paper and dried at room temperature. The loading amount of the catalyst is 0.5 mg $cm^{-2}$. Electrocatalytic experiments were carried out by the self-assembled two-electrode PME system. The anode electrolyte was 1 M KOH and the cathode electrolyte was 1 M KOH with 0.1 M $KNO_3$. The two electrolytes were cycled at 2 mL/min by the peristaltic pump (Masterflex L/S). $NO_3^-$RR was performed with chronoamperometry measurement at each fixed potential for 1 hour. The collected cathode electrolytes were diluted 5-10 times before the ammonia ($NH_3$) determination. A stability test at a current density of 100 mA/cm$^2$ was conducted in the proton exchange membrane electrolyzer for 20 hours. The volume of each electrolyte was 1.5 L. At one hour interval, 0.1 mL of cathode electrolyte was taken out for $NH_3$ determination.

**Determination of ammonia.**

The concentration of produced $NH_3$ was determined by the indophenol blue method. In detail, 2 mL of 1 M NaOH solution containing salicylic acid (5 wt%) and sodium citrate (5 wt%) was added into 2 mL of the electrolyte after the $N_2$ electrochemical reaction, followed by the addition of 1 mL of 0.05 M NaClO and 0.2 mL of $C_5FeN_6Na_2O$ (1 wt%). The absorption spectrum was measured using a UV-vis spectrophotometer. The concentration of indophenol blue was determined using the absorbance at a wavelength of 655 nm. The concentration-absorbance curve was calibrated using a standard ammonia chloride solution with a series of concentrations.

**The calculation method for Faradaic Efficiency (FE).**

The FE for $NH_3$ production was calculated at a given potential as follows:

$FE = C_{NH3} \times V \times N \times F / Q$

$C_{NH3}$: the measured $NH_3$ concentration,

V: the volume of the cathode electrolyte,

N: the number of electrons transferred for product formation, which is 8 for $NH_3$,

F: Faradaic constant, 96485 C mol$^{-1}$,

Q: quantity of the electric charge integrated by the *i-t* curve.

## Supplementary Figures

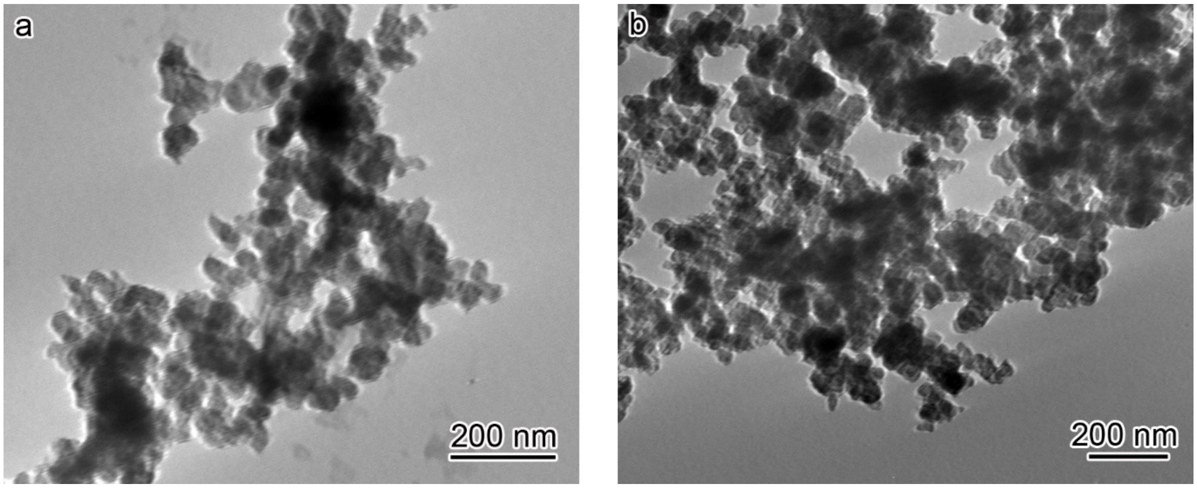

**Figure S1.** (a) TEM image of CuBr-N/CB and (b) CuI-N/CB.

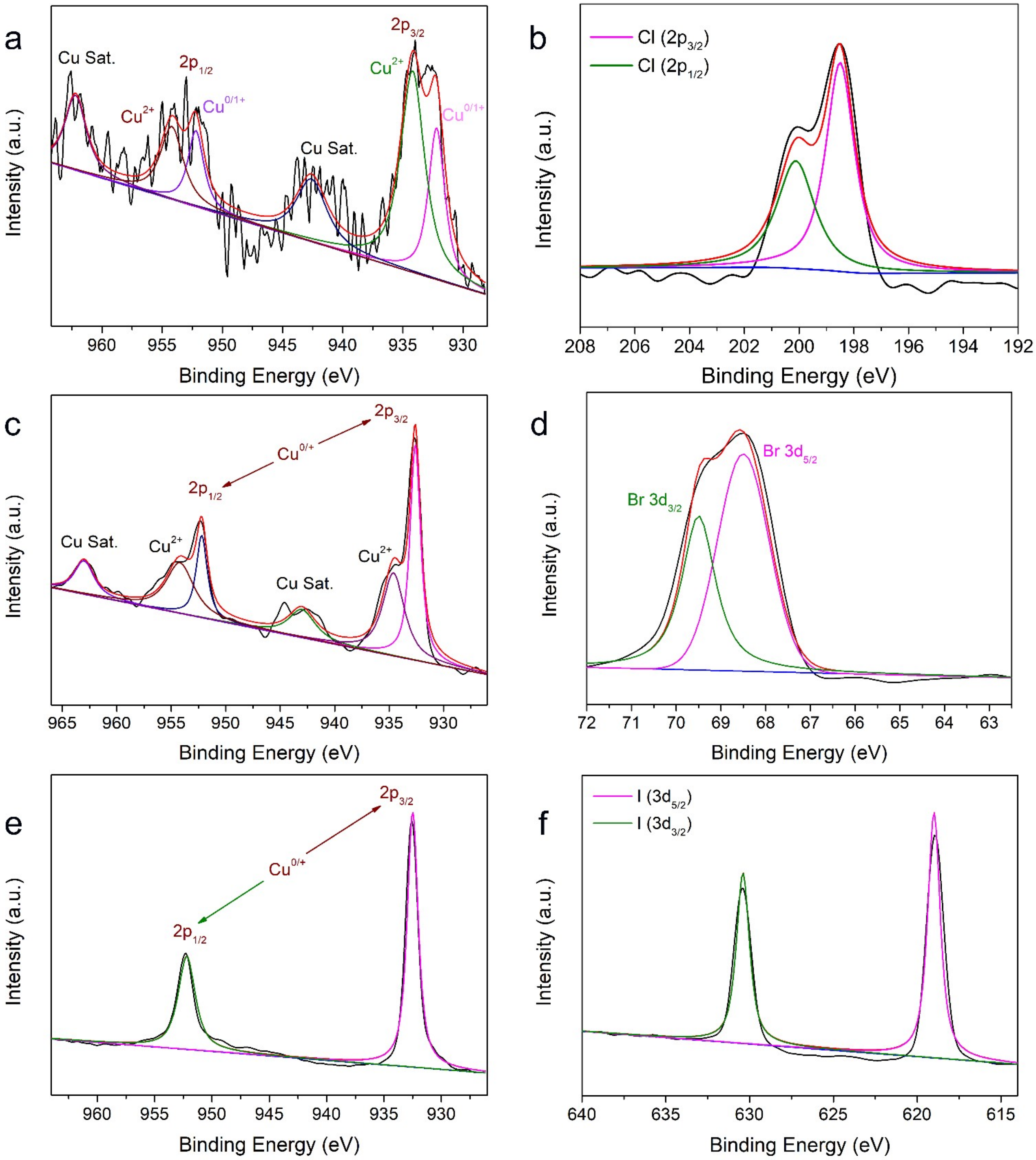

**Figure S2.** XPS spectra of (a) Cu and (b) Cl of fresh CuCl-N/CB catalyst; (c) Cu and (d) of fresh CuBr-N/CB catalyst; (e) Cu and (f) I of fresh CuI-N/CB catalyst.

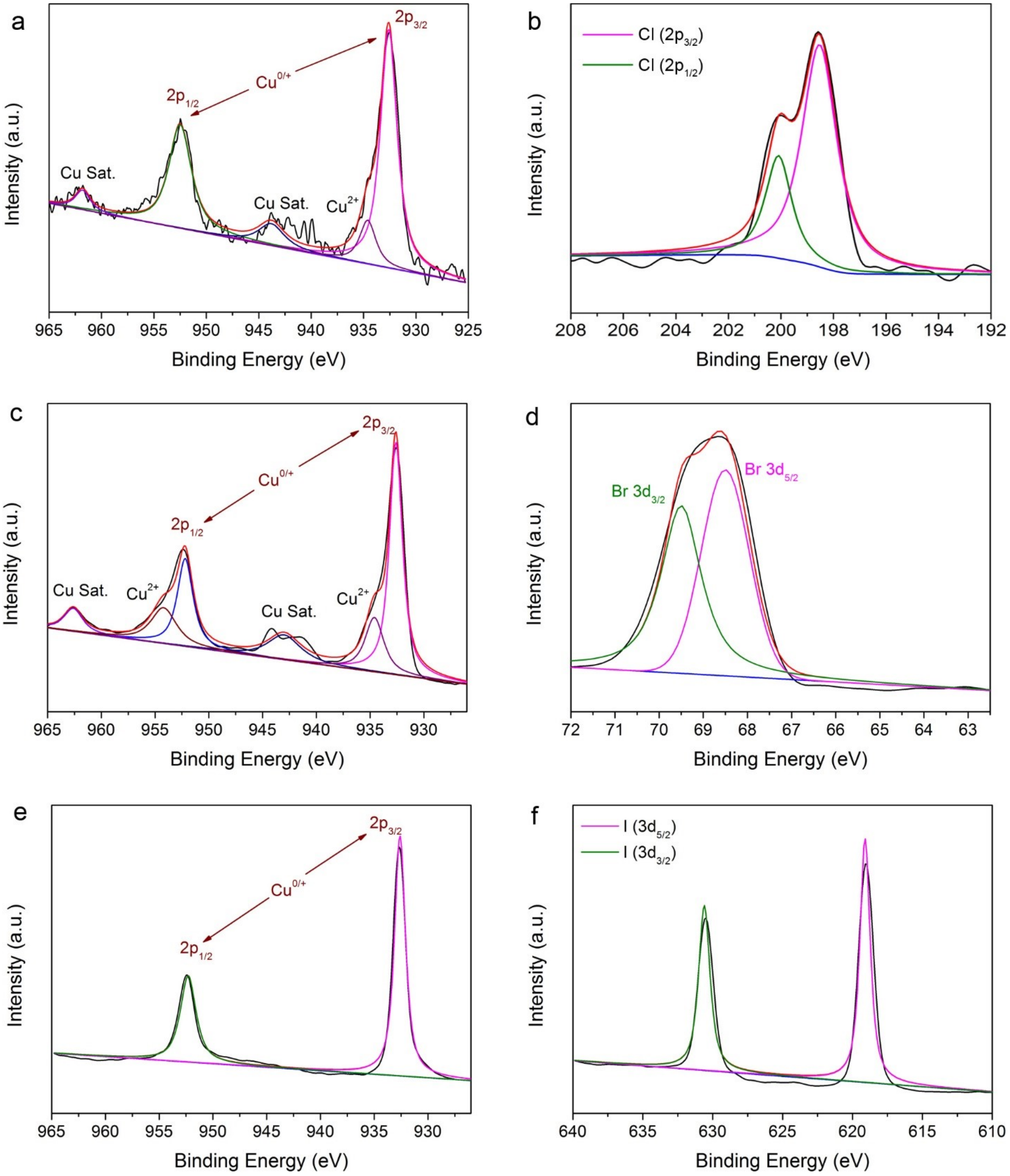

**Figure S3.** XPS spectra of (a) Cu and (b) Cl of CuCl-N/CB catalyst after 10 min CA test; (c) Cu and (d) of CuBr-N/CB catalyst after 10 min CA test; (e) Cu and (f) I of CuI-N/CB catalyst after 10 min CA test.

**Table S1.** Atomic ratio of X:Cu determined by XPS of the fresh catalysts and the catalysts after 10 min CA test.

| Atomic ratio | Cl:Cu | Br:Cu | I:Cu |
|---|---|---|---|
| Fresh catalysts | 1.51 | 2.02 | 0.71 |
| Catalysts after 10 min CA test | 1.19 | 1.07 | 0.63 |

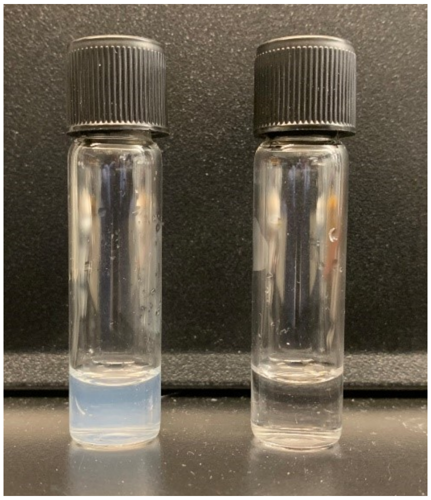

**Figure S4.** Photograph of the electrolytes after (left) and before (right) after the CA process by adding $AgNO_3$ (1 M) to precipitate $Cl^-$ using CuCl-N/CB as catalyst. $NH_3$ was removed with 80 °C heating, Excessive $HNO_3$ was added to make the electrolytes in acid condition. Here the white precipitate was AgCl.

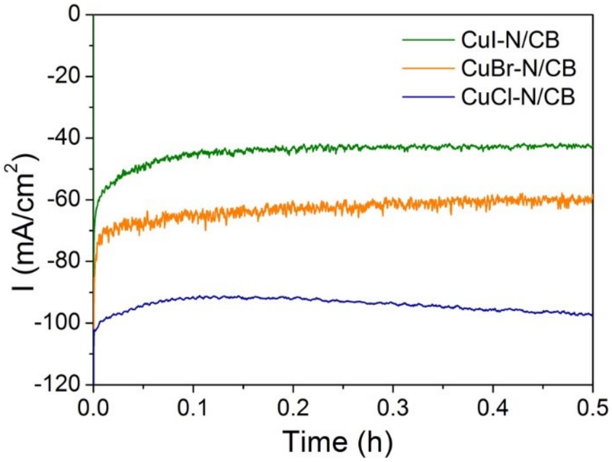

**Figure S5.** Chronoampermetric (CA) curves of CuX-N/CB at -0.76 V vs RHE.

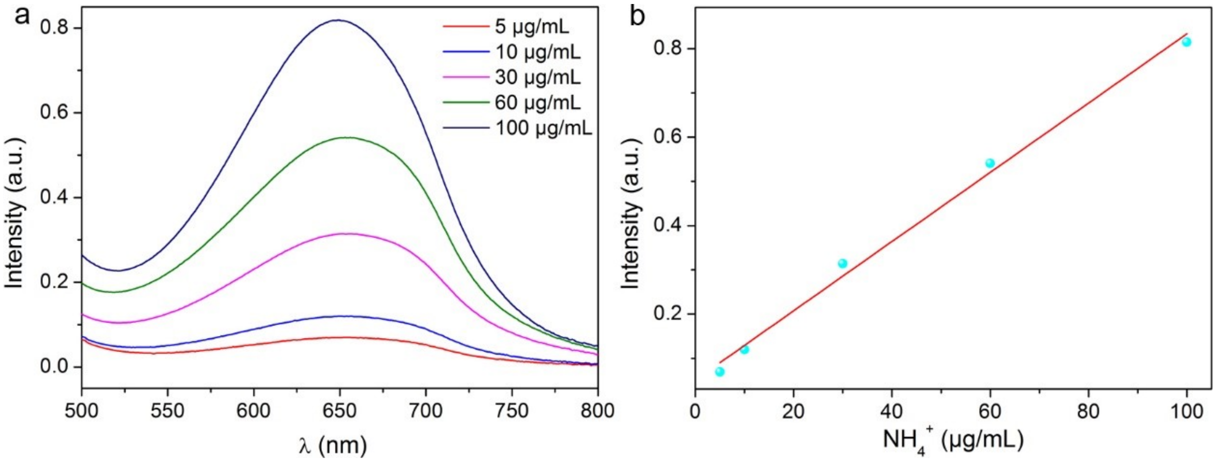

**Figure S6.** (a) UV-vis curves and (b) concentration-absorbance curve of $NH_4^+$ ions solution with a series of standard concentration. The absorbance at 655 nm was measured by UV-vis spectrophotometer. The standard curve showed good linear relation of absorbance with $NH_4^+$ ions concentration.

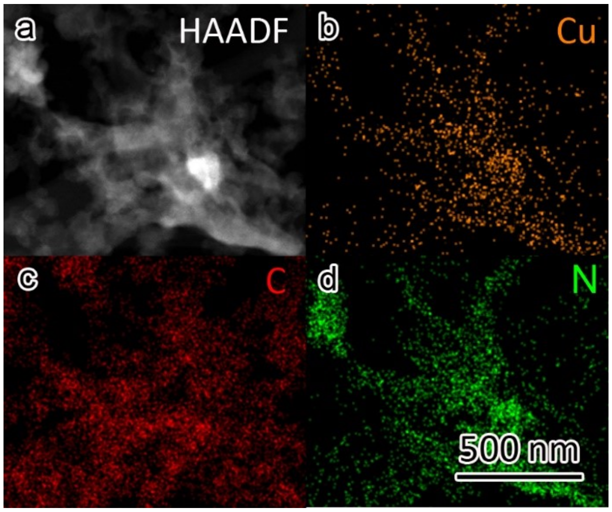

**Figure S7.** (a) HAADF-STEM and (c-d) EDS mapping images of CuCl-N/CB after the CA process, Cu (brown), C (red), and N (green).

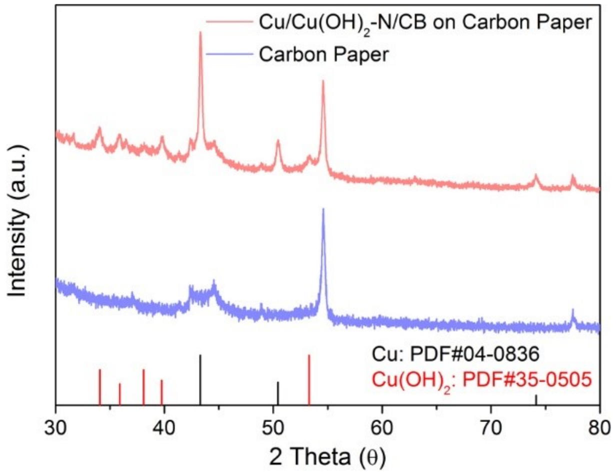

**Figure S8.** Powder X-ray diffraction pattern of carbon paper and CuCl-N/CB on carbon paper after the CA process.

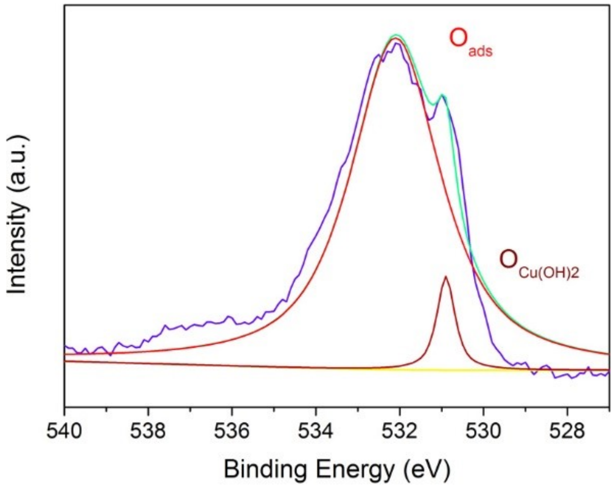

**Figure S9.** O 1s XPS spectrum of CuCl-N/CB catalyst after the CA process.

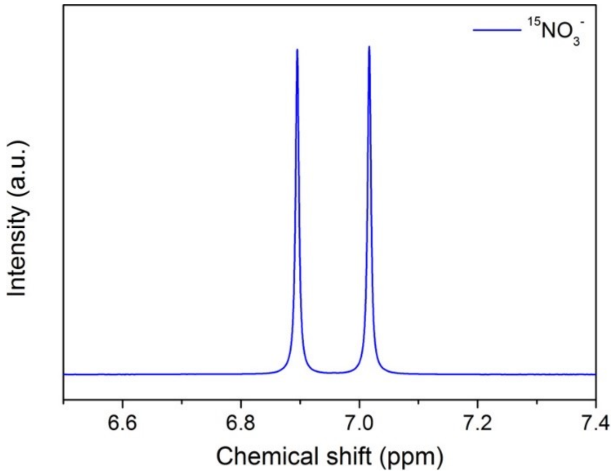

**Figure S10.** $^1H$ NMR spectra of the electrolytes after nitrate reduction at -0.76V vs RHE using $^{15}NO_3^-$ as the nitrogen source.

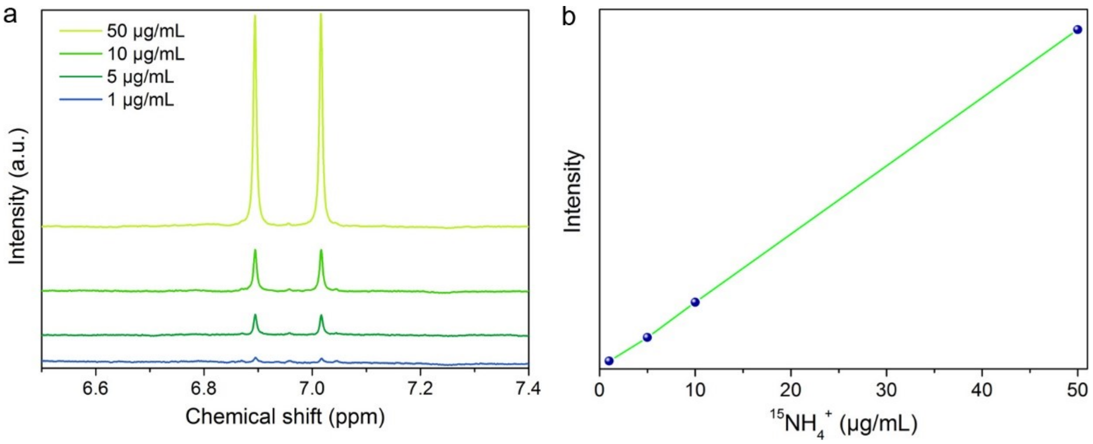

**Figure S11.** (a) $^1H$ NMR spectra of $^{15}NH_4^+$ standard solution with different concentrations. (b) $^{15}NH_4^+$ concentration-intensity standard curve. The standard curve showed a good linear relation of absorbance with $^{15}NH_4^+$ concentration.

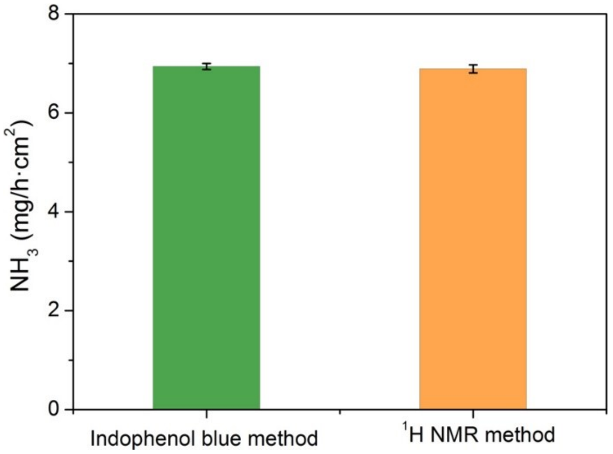

**Figure S12.** NH$_3$ yield rate of CuCl-N/CB at -0.76 V vs RHE quantified by indophenol blue method and $^1$H NMR method.

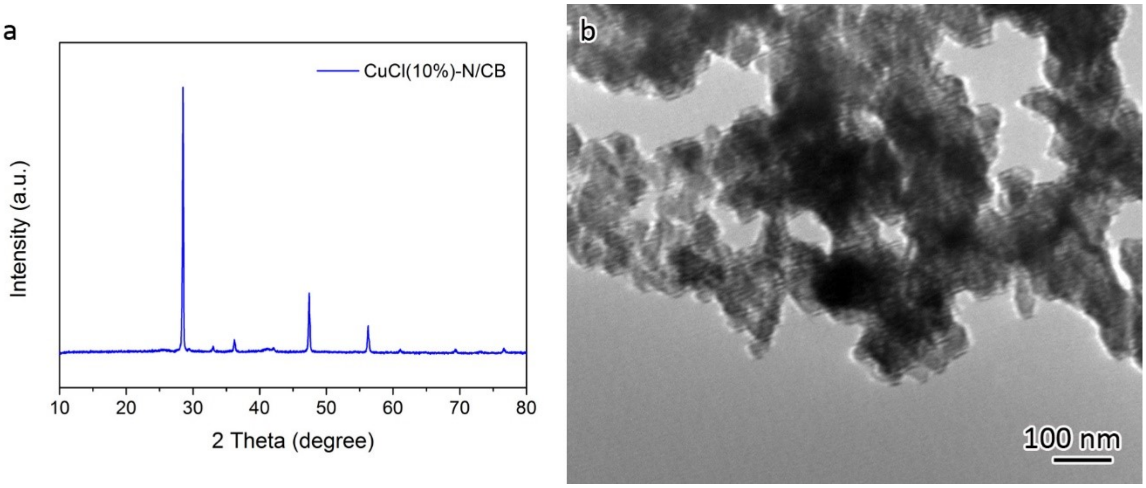

**Figure S13.** (a) Powder X-ray diffraction pattern and (b) TEM image of CuCl(10%)-N/CB.

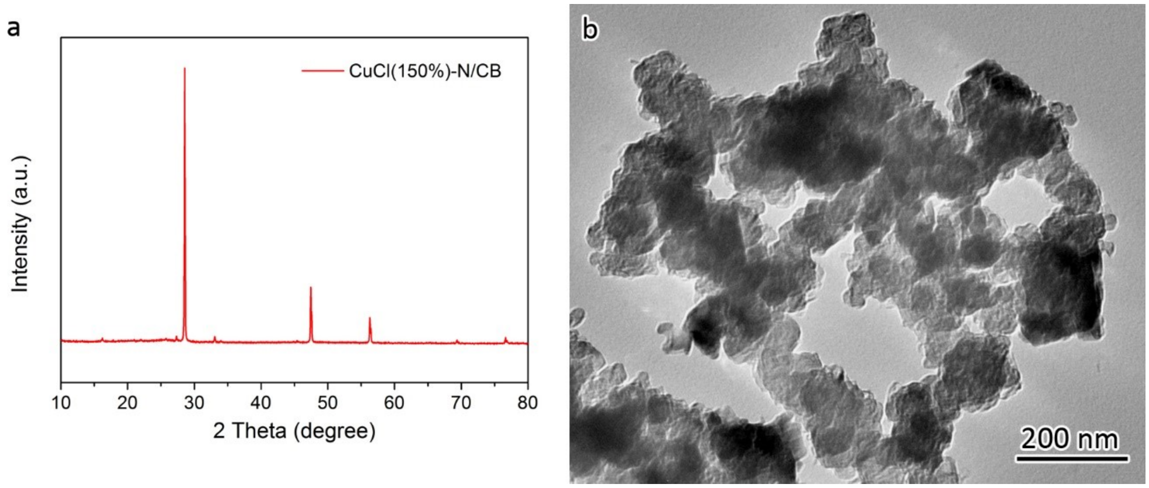

**Figure S14.** (a) Powder X-ray diffraction pattern and (b) TEM image of CuCl(150%)-N/CB.

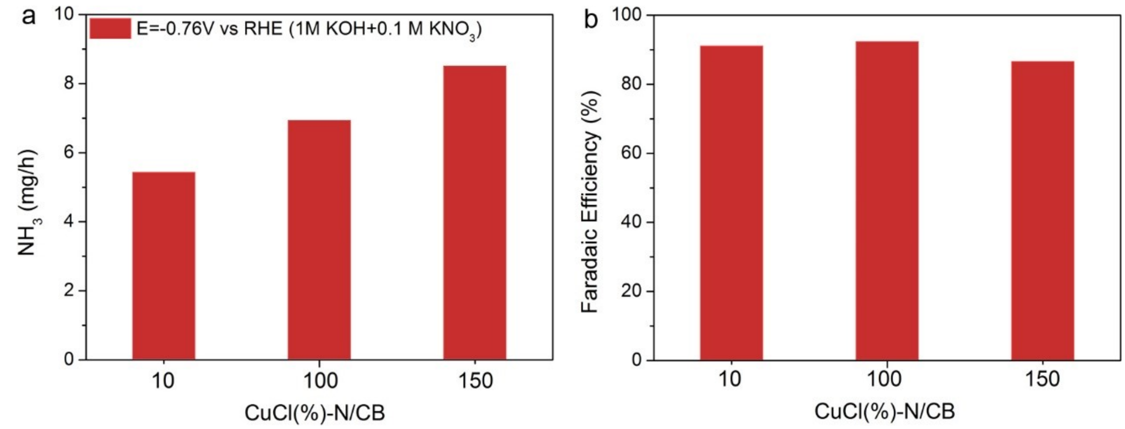

**Figure S15.** (a) $NH_3$ yield rate and (b) Faradaic Efficiency of CuCl-N/CB with various CuCl loading at -0.76 V vs RHE.

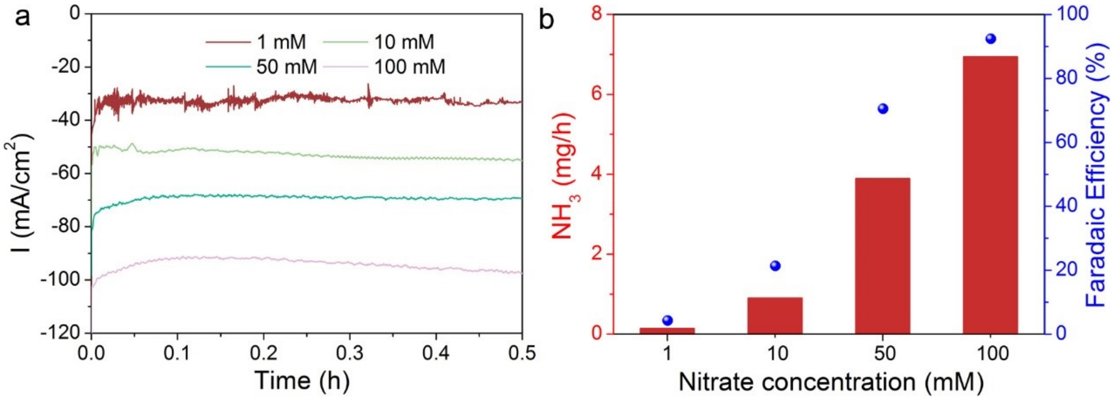

**Figure S16.** (a) CA curves and (b) $NH_3$ yield rate and FE of CuCl-N/CB with various $NO_3^-$ concentrations at -0.76 V vs RHE.

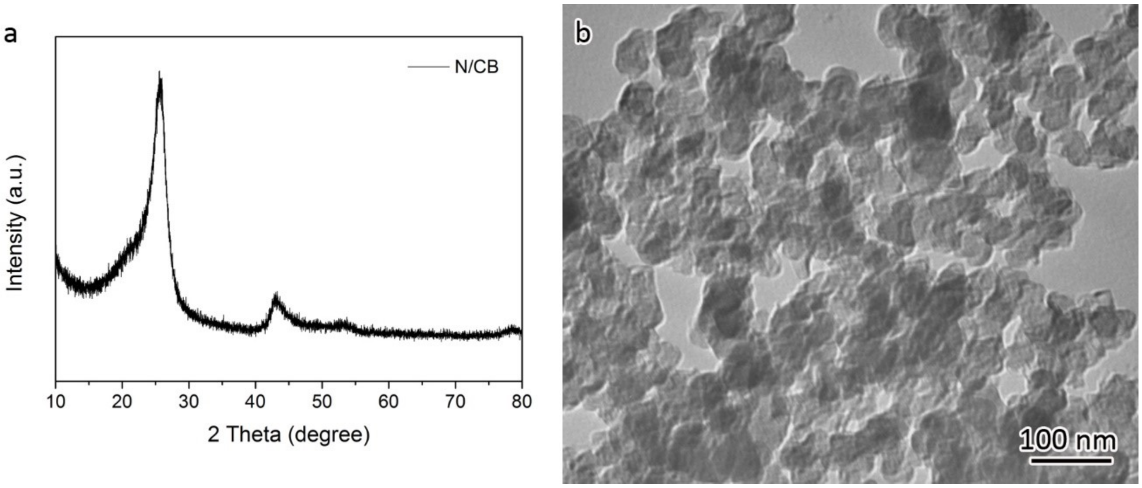

**Figure S17.** (a) Powder X-ray diffraction pattern and (b) TEM image of N/CB.

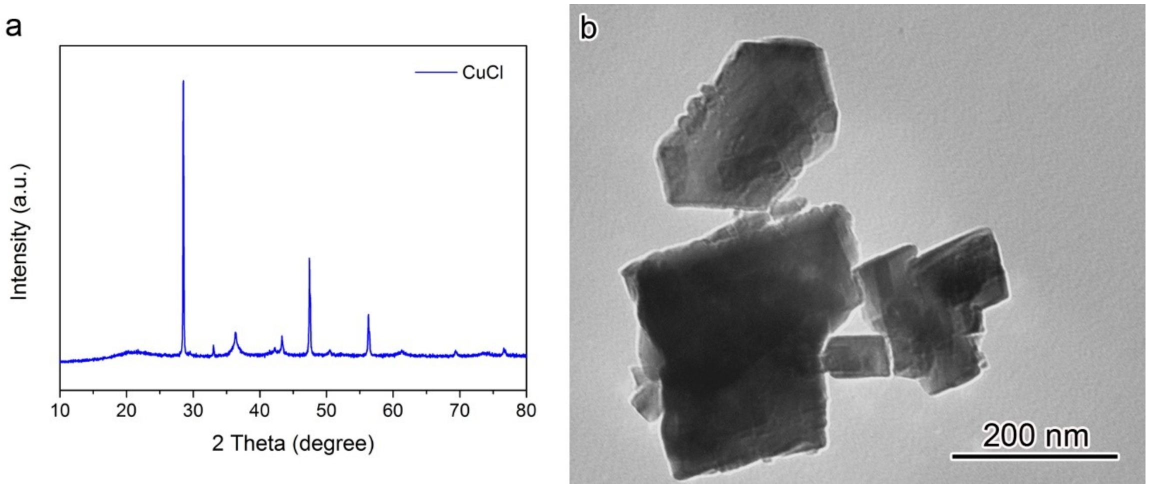

**Figure S18.** (a) Powder X-ray diffraction pattern and (b) TEM image of CuCl.

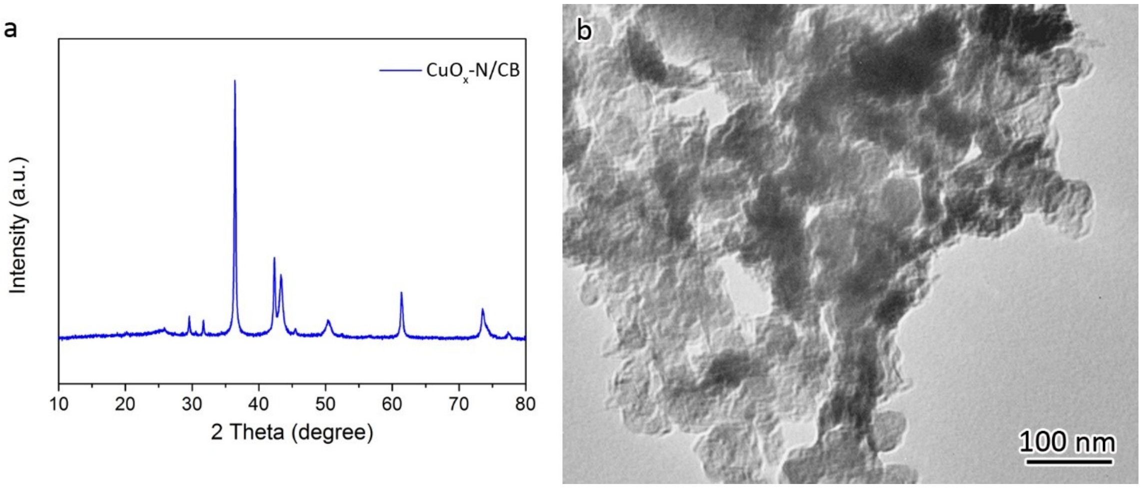

**Figure S19.** (a) Powder X-ray diffraction pattern and (b) TEM image of $CuO_x$-N/CB.

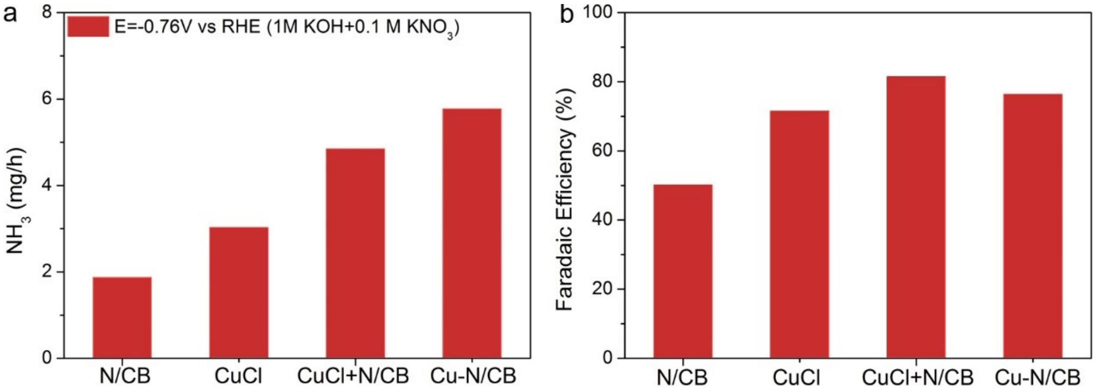

**Figure S20.** (a) $NH_3$ yield rate and (b) Faradaic Efficiency of N/CB, CuCl, CuCl+N/CB, and Cu-N/CB at -0.76 V vs RHE.

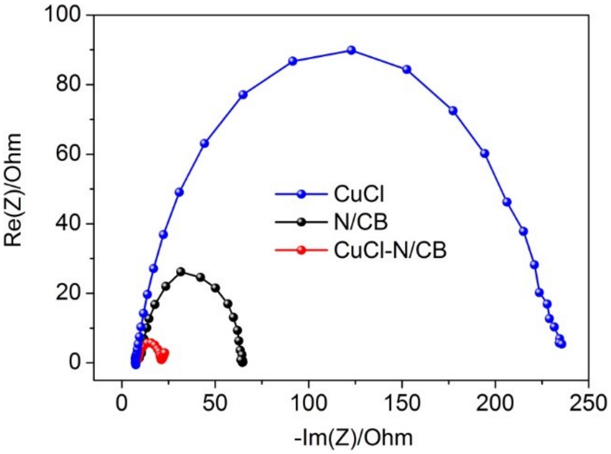

**Figure S21.** Electrochemical Impedance Spectroscopy (EIS) curves of CuCl, N/CB, and CuCl-N/CB catalysts in 1 M KOH with 0.1 M $KNO_3$.

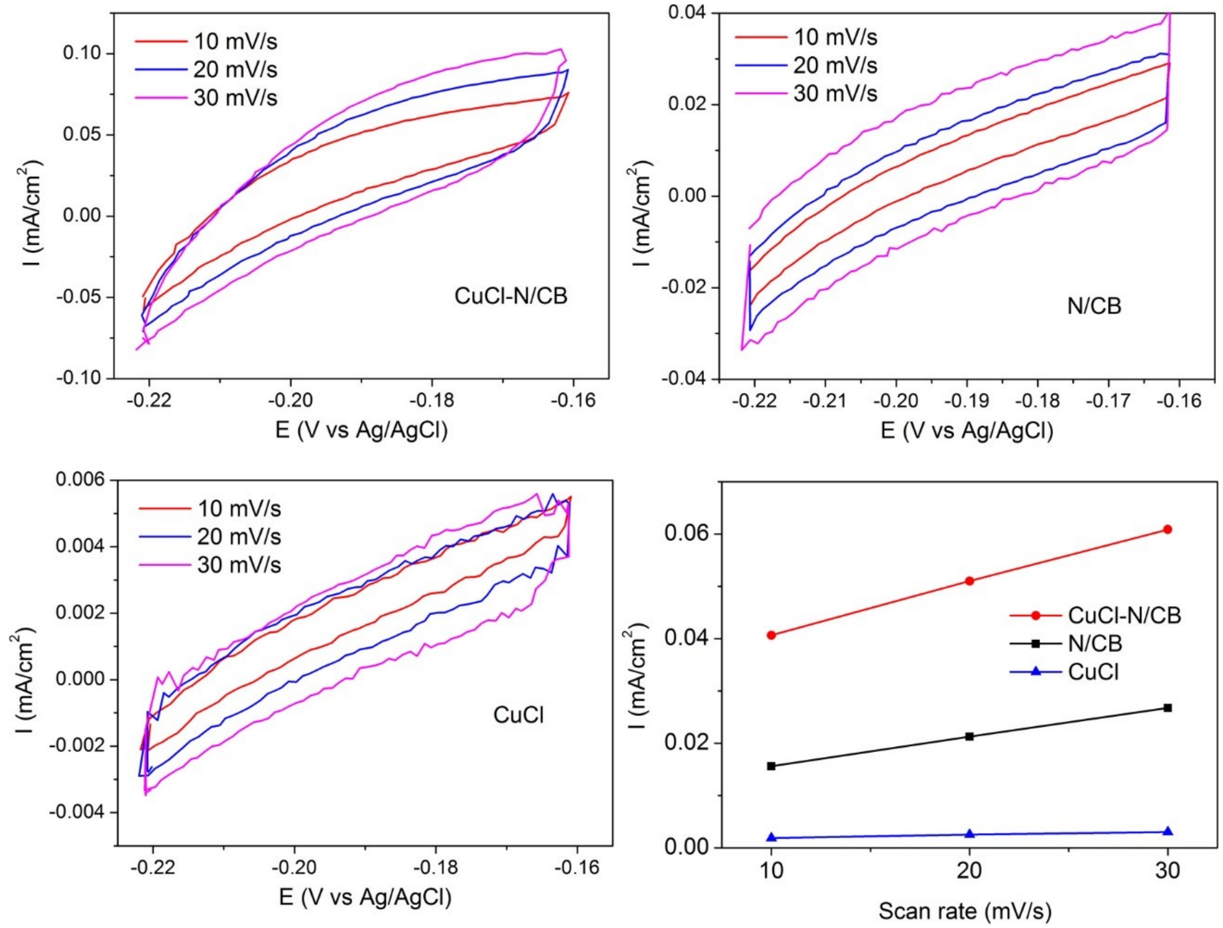

**Figure S22.** Cyclic voltammetry curves of (a) CuCl-N/CB, (b) N-CB, and (c) CuCl catalysts in 1 M KOH and 1 M KOH with 0.1 M $KNO_3$. (d) Determination of double-layer capacitance of CuCl-N/CB, N-CB, and CuCl catalysts.

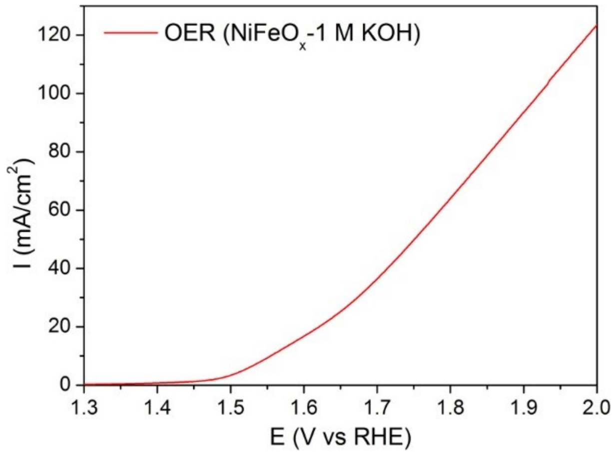

**Figure S23.** Liner sweep voltammetry curve of $NiFeO_x$ catalyst in 1 M KOH electrolyte.

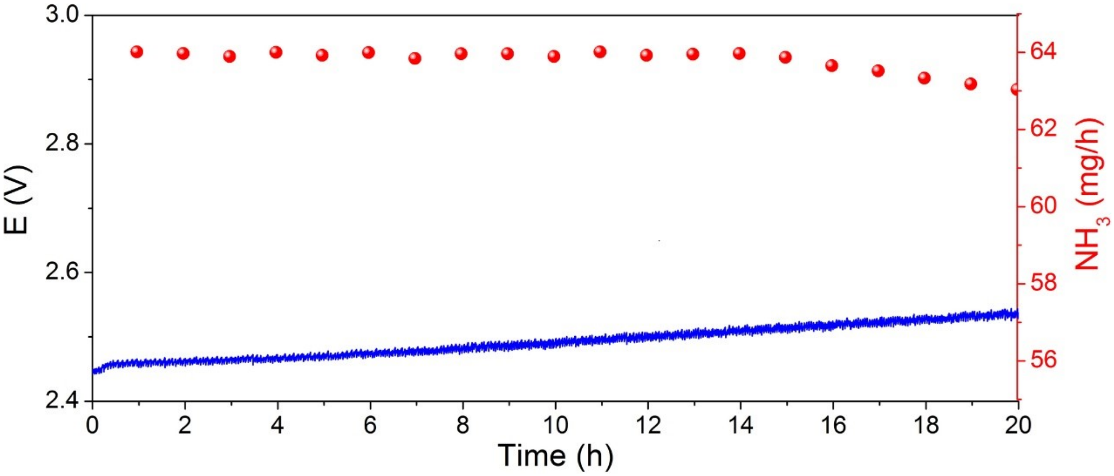

**Figure S24.** Stability test at a current density of 100 mA/cm$^2$ and the corresponding $NH_3$ yield rate at one hour interval in the PEM reactor.

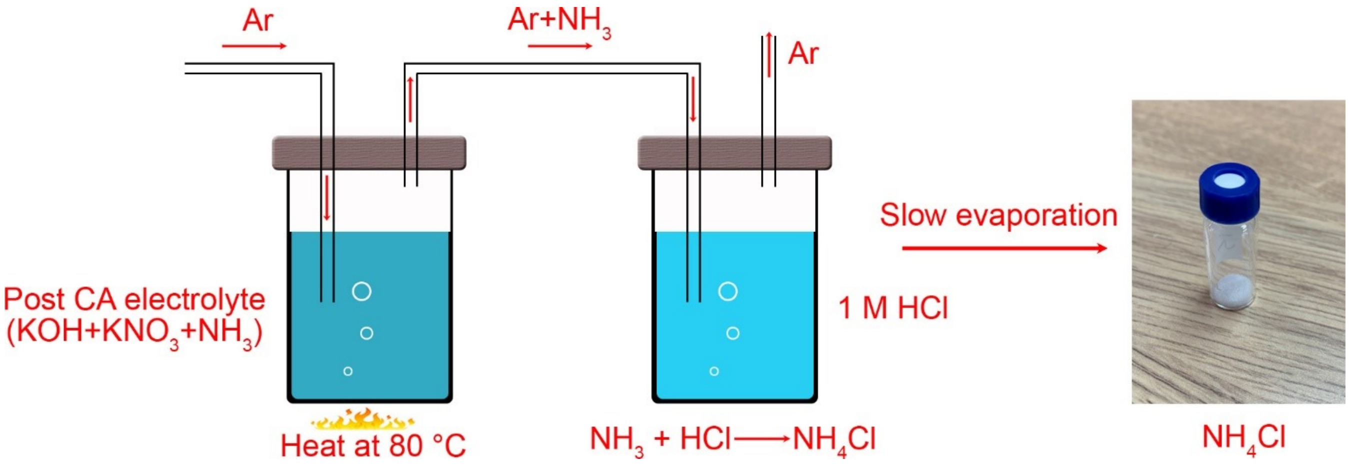

**Figure S25.** Systematic illustrating the acid stripping process to trap $NH_3$ and generate $NH_4Cl$ powder.

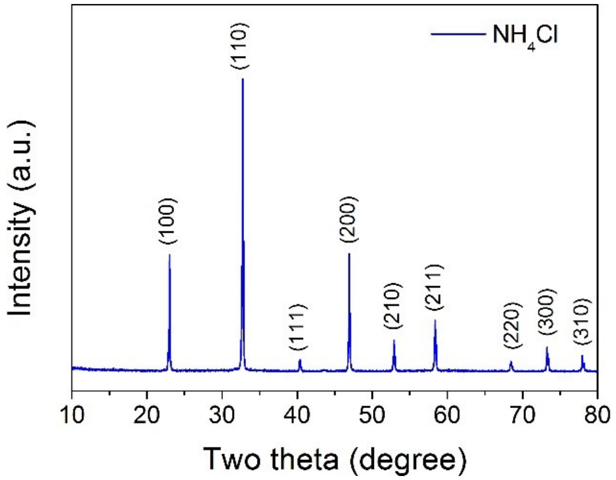

**Figure S26.** Powder X-ray diffraction pattern of $NH_4Cl$ powder.